Drug Metabolism and Disposition

SUPPLEMENTAL MATERIAL

Immobilized Cytochrome P450 for Monitoring of P450-P450 Interactions and Metabolism

Bostick C.D., Hickey K.M., Wollenberg L.A., Flora D.R., Tracy T.S., & Gannett P.M.

Department of Pharmaceutical Sciences, School of Pharmacy, West Virginia University, Morgantown, West Virginia (CB, KH)

Array BioPharma, Boulder, Colorado (LW)

Department of Experimental and Clinical Pharmacology, College of Pharmacy, University of Minnesota, Minneapolis, Minnesota (DF)

College of Pharmacy, University of Kentucky, Lexington, KY (TT)

Department of Pharmaceutical Sciences, College of Pharmacy, Nova Southeastern University, Ft. Lauderdale, Florida (PG)

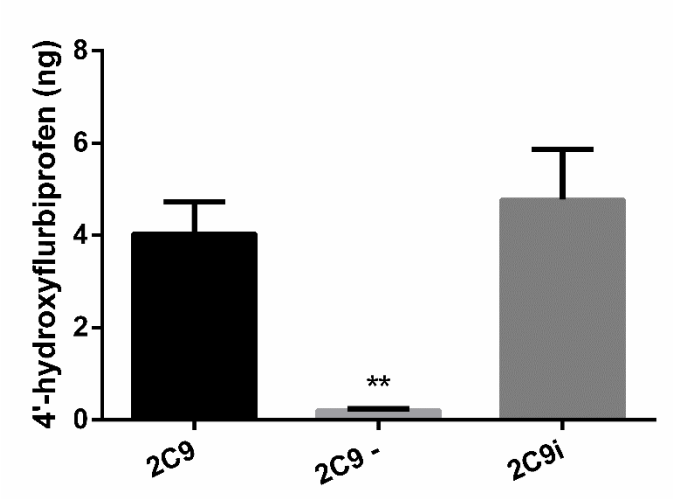

Supplemental Figure 1. Comparison of metabolism between lipid reconstituted CYP2C9 (2C9) and Immobilized CYP2C9 (2C9i) at the same weight by volume metabolic incubation. 2C9- represents a negative control were NADPH was omitted, and thus results in significantly reduced metabolism. Ratios of CPR:P450 (8:1) are the same as used in all presented CYP2C9i runs.

Supplemental Table 1 CYP2C9 regions of interest and the relevant residues.

Region of Interest	CYP2C9 Residues
Substrate Access Channel[a]	P37 I42 I45 I47 F69 K72 I74 R97 G98 I99 P101 L102 A106 R108 G109 P211 N218 P221 I222 H230 V237 288
Solvent Channel[a]	C206 E300 R307 F476
CPR Binding Site[b]	K84 D89 E92 K121 R125 R132 K270 K273 K421 K423 K432 E438
P450 Binding Site on CPR[c]	D208

[a](Cojocaru *et al.*, 2011b)
[b](Hazai *et al.*, 2005)
[c](Shen and Kasper, 1995; Hamdane *et al.*, 2009)

CYP2C9 Structures Approximate a Range of Open-closed Conformations. Several CYP2C9 crystal structures were examined: 1OG2 (without substrate), 1OG5 (with bound warfarin) (Williams *et al.*, 2003), and 1R9O (with bound flurbiprofen) (Wester *et al.*, 2004). Assessment of structural similarity reveals that the models are largely identical with Qres values > 0.8 in all regions except for the area surrounding substrate access channels to the active site (Supplemental Figure 1). When Q = 1, the structures are identical, as Q approaches 0 the structures are increasingly dissimilar. The 1OG2 and 1OG5 models, intended to represent open and closed states respectively, were more structurally similar to each other than to 1R9O, a partially open conformation. Therefore further analysis was conducted only on the 1OG5 (closed) and 1R9O (partially open) models. According to the energetically favorable models returned by

GRAMM, both conformations are capable of forming dimers with CPR in solution, though the most energetically favorable CPR binding orientations resultant from the blind docked model do not include an orientation in which electron transfer normally functions. However, the closest match occurred between a partially open CYP2C9 and CPR, crystallized in this model with a bound flurbiprofen, but in a conformation more closely related to P450 enzyme in the absence of substrate. This result is interesting because it is slightly at odds with the P450 catalytic cycle, in which the first electron transfer, and thus presumably CPR binding, does not occur until after the substrate has bound.

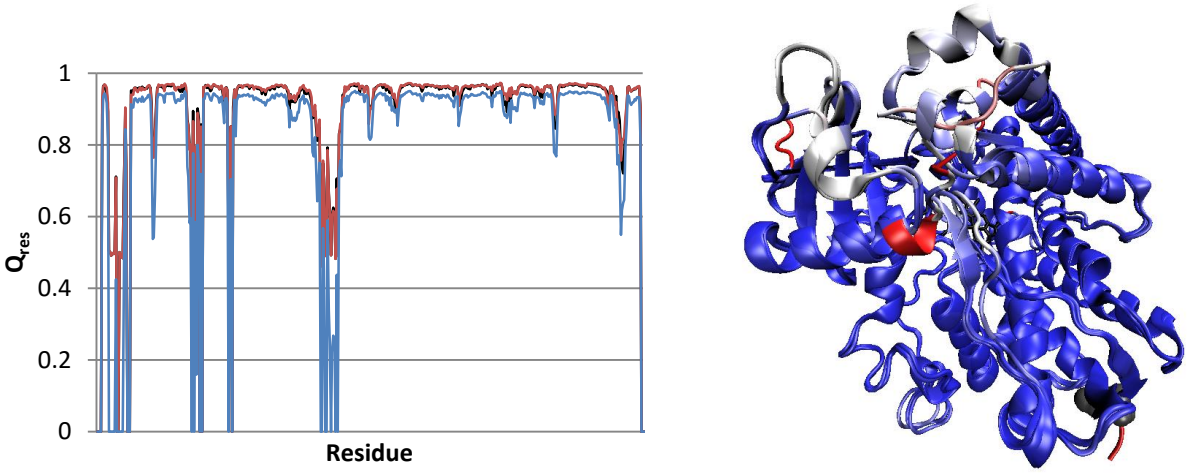

Supplemental Figure 2. Left: Qres values for CYP2C9 crystal structures 1OG2 (black), 1OG5 (red), 1R9O (blue). Most regions of the CYP2C9 molecules were structurally similar with Qres values > 0.8. Regions of greater structural differences surrounded the substrate channels to the active site. Smaller structural differences exist between 1OG2 and 1OG5 CYP2C9 than with 1R9O CYP2C9. Right: Structural alignment of CYP2C9 molecules. Three CYP2C9 molecules, PDB ID 1OG2, 1OG5, and 1R9O, were used in analysis of dimerization location and strength. These molecules were structurally similar (blue) in all regions except that surrounding the entrance to the active site (white). Areas shown in red are present in only one of the three crystal structures. The N-terminus and central heme group have been colored black for spatial reference.

		Active Site Access Tunnel(s)									
		1	2	3	4	5	6	7	8	9	10
	2C9									><	
	3A4		<		<						
	2D6	>					>				
1R9O	CPR				>		>		>		
	2C9	<<						>			
	3A4										
	2D6										
1OG5	CPR								<		

		Solvent Access Tunnel(s)									
		1	2	3	4	5	6	7	8	9	10
	2C9							>	<		
	3A4						>	>			
	2D6									>	>
1R9O	CPR	>	<	>				>			
	2C9		>>	>>		>>			>>	>>	>>
	3A4		>		>	>			>	>	
	2D6		>	>						>	
1OG5	CPR			>	>	<	>	<		>	

		CPR binding site									
		1	2	3	4	5	6	7	8	9	10
	2C9			>			>				
	3A4									<	
	2D6				>						
1R9O	CPR										
	2C9										
	3A4							<			
	2D6								>		
1OG5	CPR										

		N-terminus									
		1	2	3	4	5	6	7	8	9	10
	2C9				>						>
	3A4								>		
	2D6										
1R9O	CPR										
	2C9										
	3A4										
	2D6									<	
1OG5	CPR										

Supplemental Table 2. Dimer binding sites predicted by GRAMMX. Each of the ten models returned by GRAMMX was examined. Those with an interface in the indicated area and that involved 40% or greater of the residues listed in Table 1 for the area are denoted with a '>', those with interface areas involving less than 40% of the residues indicated for an area of interest are denoted with a '<'. The homodimer models that have multiple demarcations are affecting the regions of interest of both partner molecules.

CPR Binding Site as Predicted by STAMP Structural Alignment. The CYP2C9 CPR binding site has been previously reported (Hazai *et al.*, 2005). Both the closed and partially open models of CYP2C9 were structurally aligned with the crystal structures used for CYP2D6 and CYP3A4. Residues involved in the CYP2C9 CPR binding site were mapped onto the CYP2D6 and CYP3A4 molecules. Those with Qres values greater than 0.75 are reported (Table S2).

CPR Binding Site												
CYP2C9	E92	R125	R132	K421	K432	K84	D89	K121	K270	K273	K423	E438
CYP3A4	Y99		T138		P439	K91	K96	K127			P429	M445
CYP2D6	E96	R133	R140	K429	R440	R88	T93	R129	E278	K281	E431	E446

*Supplemental Table **3**. Residues involved in CYP2C9 CPR binding were mapped onto CYP3A4 and CYP2D6. Those residues exhibiting strong structural similarity with Qres values greater than 0.75 are reported. CYP2C9 residues listed in the right hand side of the table were reported in the CYP2C9-CPR interface for multiple models, those on the left were reported for a single model.*

Enzyme Attachment and Characterization by SPR. Surface plasmon resonance (SPR) is a technique that measures the change in resonance angle of light to excite surface plasmons on a reflective thin film

sample. Changes in resonance angle occur when the local refractive index changes, for example, upon ligand-analyte interaction, or more generally, changes in local mass density of the sample surface. CYP2C9 was immobilized to a planar gold surface via a self-assembled monolayer (SAM) reproducibly achieving immobilization levels of 70-200 response units relative to the ethanolamine capped control surface. This low immobilization level was targeted in order to allow kinetic measurements of the system (Karlsson *et al.*, 1991; Myszka, 1999).

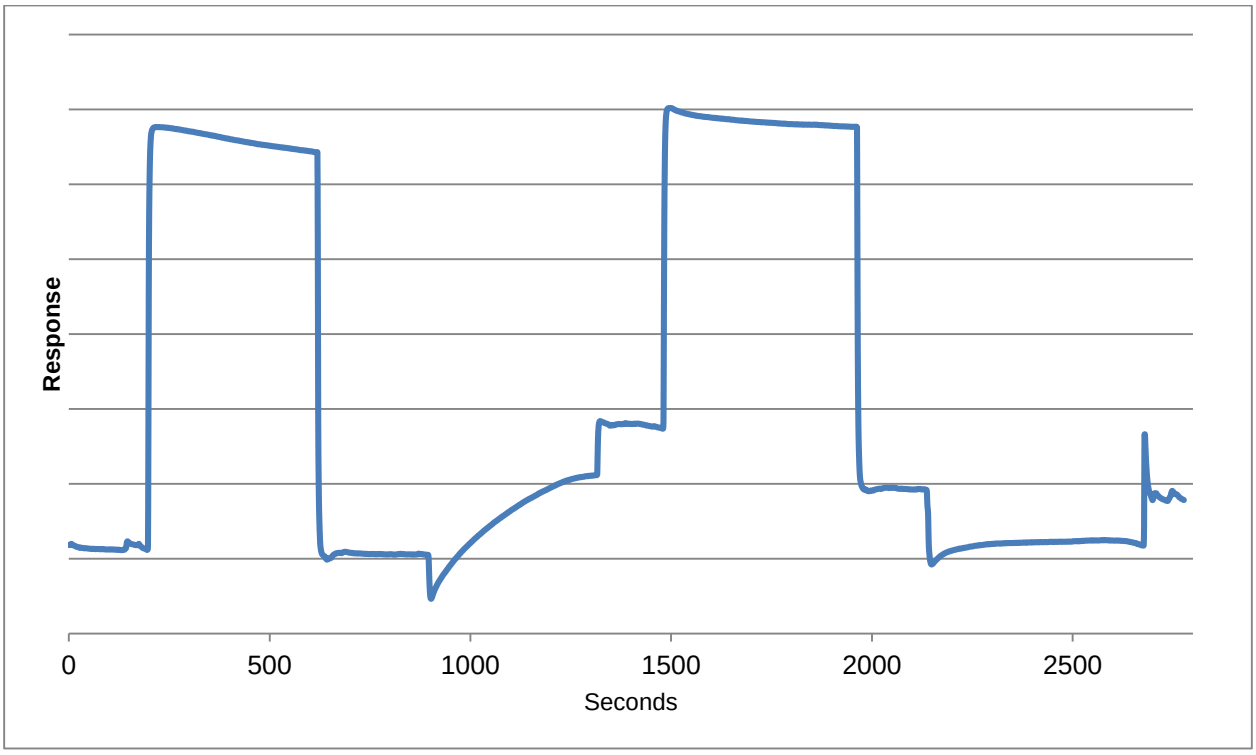

Supplemental Figure 3. Representative sensorgram of CYP2C9 immobilization using surface plasmon resonance. Final increase in response reflect addition of mass onto the surface of the SAM functionalized chip due to immobilization of CYP2C9. Using a HEPES running buffer from time = 0 s the platform is subjected to EDC/NHS to activate the carboxylic acid groups in the SAM (t = 140 s), CYP2C9 (t = 900 s), ethanolamine to cap the unreacted NHS-esters (t = 1490 s), and finally washed with CTAB to remove any non-specifically binding P450 molecules (t = 2140 s).This procedure is followed in a control flow cell, on the same SPR chip, with the reversal of the ethanolamine and CYP2C9 injections, which should block immobilization of CYP2C9 by EDC/NHS coupling. This ensures both control (no CYP2C9 Immobilized) and active flow cell (CYP2C9 immobilized) are subjected to identical conditions. The immobilized response was calculated from the final response level – baseline response of the control flow cell subtracting the values observed in the reference flow cell.

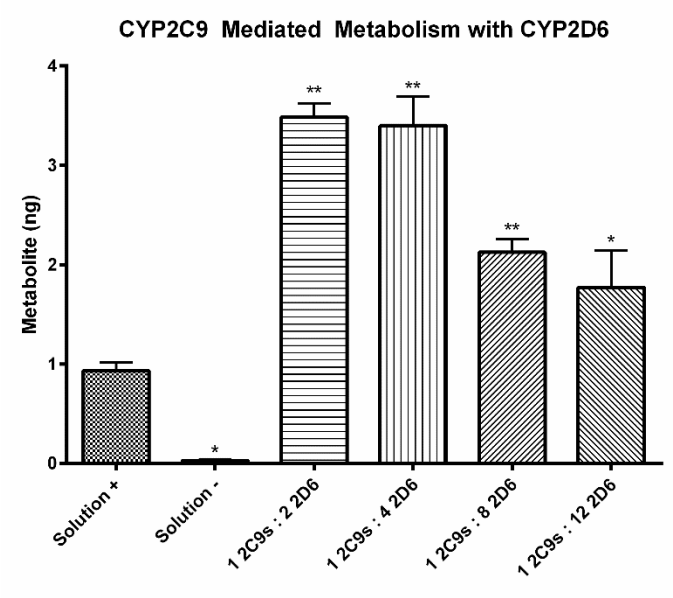

Supplemental Figure 4. Effect of CYP2D6 on CYP2C9-mediated flurbiprofen metabolism at four ratios of 2C9s to CYP2D6 with saturating CPR (1 total P450 :10 CPR). Solution + and Solution – represent controls with CYP2C9 (.25 nM) incorporated in lipid with Solution – omitting NADPH and thus producing little to no metabolite. A significant activation ($p < .01$) is seen at CYP2C9:CYP2D6 ratios of 1:2 to 1:8. This activation is reduced slightly at a ratio of 1:12 ($p < .05$). Single-factor analysis of variance was used for statistical comparisons.

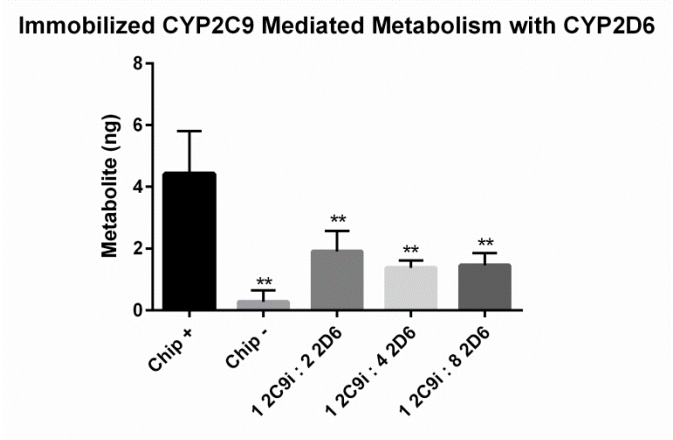

Supplemental Figure 5. Effect of CYP2D6 on immobilized CYP2C9-mediated flurbiprofen metabolism at three ratios of 2C9i to lipidless CYP2D6 with saturating CPR (1 total P450 :10 CPR). Chip + and Chip – represent controls with (–) omitting NADPH and thus producing little to no metabolite. A significant inhibition ($p < .01$) is seen at CYP2C9i:CYP2D6 ratios of 1:2 and higher. Single-factor analysis of variance was used for statistical comparisons.